

Electrochemical Simultaneous Detection of Paracetamol and 4-aminophenol Based on bis-Schiff Base Cobalt Complex

Qiuqun Liang¹, Zheng Liu^{1,*}, Chuxin Liang¹, Guo-Cheng Han^{2,*}, Shufen Zhang^{1,3}, Xiao-Zhen Feng²

¹ College of Chemical and Biological Engineering, Guilin University of Technology, Guangxi Guilin 541004, P.R. China

² School of Life and Environmental Sciences, Guilin University of Electronic Technology, Guilin 541004, P.R. China

³ Key Laboratory of fine chemical engineering of Dalian University of Technology, Dalian, 116024, P.R. China

*E-mail: lisa4.6@163.com, hancg1981@163.com

Received: 7 January 2019 / Accepted: 15 May 2019 / Published: 30 June 2019

A simple and sensitive method was proposed for the simultaneous detection of paracetamol (acetaminophen, PR) and 4-aminophenol (4-AP) based on bis-Schiff bases and their cobalt complexes modified glassy carbon electrode. Bis-Schiff bases, namely 2,6-diaminopyridine-o-carboxyl benzaldehyde (L1), 2,6-diaminopyridine-m-carboxyl benzaldehyde (L2), 2,6-diaminopyridine-p-carboxyl benzaldehyde (L3) and their cobalt complexes (noted as C1, C2 and C3) were synthesized and characterized by MS, IR, UV-Vis, fluorescence spectra and thermogravimetric analysis, which were used for modification of glassy carbon electrode by electrodeposition method. The electrochemical behaviors of PR and 4-AP on the modified electrode were studied by cyclic voltammetry. The results showed C1 modified electrode exhibited excellent electro-catalytic activities, high selectivity and sensitivity towards oxidation of PR and 4-AR than that of bare glassy carbon electrode, C2 and C3 modified electrodes. The corresponding differential pulse voltammetry (DPV) current signals appeared as two well resolved oxidation peaks, with peak potential differences of 0.31 V (PR and 4-AR). For simultaneous detection, linear responses for PR and 4-AR were obtained under optimal conditions in the following concentration ranges: 5 to 30 $\mu\text{mol}\cdot\text{L}^{-1}$, with detection limits of 1.86 and 2.08 $\mu\text{mol}\cdot\text{L}^{-1}$, respectively. These results demonstrated that C1 modified glassy carbon electrode can be a promising electrochemical sensor for electrocatalytic applications, which was proved to be applicable for simultaneous detection of PR and 4-AR in paracetamol tablets.

Keywords: Schiff base cobalt complexes; modified electrode; simultaneous detection; acetaminophen; 4-aminophenol

1. INTRODUCTION

Drugs can treat diseases, but also have adverse reactions to humans. The contents of active and bad components of drugs can be obtained by drug analysis, which can improve the efficacy and safety of drug use, and reduce the cost and risk of drug treatment [1,2]. Paracetamol, alias acetaminophen (PR), which has been used as an analgesic for more than 30 years, is considered to be an effective antipyretic for fever and pain in adults and children [3]. However, excessive accumulation of toxic metabolites of PR may lead to severe or even fatal liver toxicity, pancreatitis and rashes [4]. 4-aminophenol (4-AP) is the main hydrolytic degradation product of PR. Because of its nephrotoxic teratogenicity, 4-AP is not allowed to exist in large quantities in drugs [5,6]. Therefore, it is necessary to determine 4-AP and PR simultaneously.

So far, there have been several methods for simultaneous detection of PR and 4-AP, such as high performance liquid chromatography (HPLC) [7,8], voltammetry [9], titration [10], capillary electrophoresis [11], fluorescence spectrophotometry [12] and spectrophotometry [13,14]. However, these methods are expensive, cumbersome and time-consuming. Owing to PR and 4-AP are electroactive compounds, people have a keen interest in the development of chemically modified electrodes [15-20]. Wang and co-workers [4] used palladium/graphene oxide and gold nanoparticles as electron mediators to prepare Au/Pd/rGO electrochemical sensors for the detection of acetaminophen and 4-aminophenol in actual samples. The electrochemical sensor was found to have good electrocatalytic activity for the redox of acetaminophen and 4-aminophenol. Poomrat and co-workers [17] used a graphene-polyaniline as an electronic medium to modify a glassy carbon electrode to prepare a novel electrochemical droplet microfluidic device with high active surface area and electrochemical conductivity, determination of paracetamol and 4-aminophenol in the drug. Hayati and co-workers [21] prepared a modified glassy carbon electrode using poly(2,2-(1,4-phenylenedivinylidene)bis-8-hydroxyquinoline) as an electron mediator, at the same time, acetaminophen and 4-aminophenol were detected in drugs and urine, and the modified electrode was found to have higher selectivity to acetaminophen with excellent sensitivity and stability. Yin and co-workers [22] prepared a modified glassy carbon electrode using gold nanoparticles and sodium lauryl sulfate modified layered double hydroxide as an electron medium, and simultaneously determined acetaminophen, dopamine and 4-aminophenol, the modified electrode was found to exhibit excellent redox activity on the test substance. In addition, Yin and co-workers [23] used CdSe microspheres as an electronic medium to prepare modified glassy carbon electrodes, studied the behavior of phenacetin on the electrodes, and simultaneously determined acetaminophen and 4-aminophenol. It was found that CdSe microspheres have excellent adsorption and catalytic ability, which can significantly improve the electrochemical response of phenacetin, acetaminophen and 4-aminophenol, in the presence of multiple substances. Leandro Yoshio and co-workers [24] prepared a microfluidic paper-based electrochemical detection device that is inexpensive to produce, simple and sensitive, and can simultaneously measure acetaminophen and 4-aminophenol. Tony and co-workers [25] electropolymerized Patton and Reeder's on a carbon paste electrode and determined acetaminophen, which was also undisturbed in the presence of 4-aminophenol.

The chemically modified electrode has the advantages of easy preparation, good sensitivity, high chemical stability, large response signal, etc. It is an important means for food analysis [26], drug

detection [27], water sample detection [28], etc. The Schiff bases and their metal complexes have good antitumor, antibacterial, antioxidation and antiviral activities, and have good application prospects in the fields of chemical catalysis, biomedicine, functional materials, food industry, and they also play an important role in the field of electrochemistry [29-35]. Transition metal complexes, due to their variable valence, can participate in electron transfer and redox processes, so they are often used as electronic media for modified electrodes [36,37], it can improve the selectivity and sensitivity of electrochemical detection. Köse and coworkers [38] synthesized two Schiff base compounds N,N'-Bis (2-methoxyphenylene)-1,5-diaminonaphthalene and N,N'-Bis (3,4,5-trimethoxybenzylidene) -1,5-diaminonaphthalene, and the sensor properties of two Schiff base compounds was characterized by the analytical and spectroscopic methods. Kumar and co-workers [39] synthesized a series of acyclic Schiff base chromium II and I complexes by microwave irradiation, and attempted to manufacture a novel modified electrode based on the complexes for the determination of catechol. Shi and co-workers [27] used solid-state carrier material carboxylic acid resin beads to prepare an immunosensor and successfully detected diclofenac in actual water samples. Shiju and co-workers [28] synthesized the 4-amino antipyrine derivative platinum complex Schiff base, and studied its biological activity, providing an important method for the diagnosis and treatment of cancer in the medical community.

In this study, firstly, 2,6-diaminopyridine was used as the starting material, and anhydrous ethanol was used as the solvent to react with o-carboxybenzaldehyde, m-carboxybenzaldehyde and p-carboxybenzaldehyde to form 2,6-diaminopyridine-o-carboxyl benzaldehyde (L1), 2,6-diaminopyridine-m-carboxyl benzaldehyde(L2) and 2,6-diaminopyridine-p-carboxyl benzaldehyde (L3), respectively. Secondly, the above obtained products were reacted with cobalt acetate to form 2,6-diaminopyridine-o-carboxyl benzaldehyde Bis-schiff base cobalt complex (C1), 2,6-diaminopyridine-m-carboxyl benzaldehyde bis-schiff base cobalt complex (C2) and 2,6-diaminopyridine-p-carboxyl benzaldehyde bis-schiff base cobalt complex (C3), respectively. Structure and properties of synthetic bis-schiff base and their complexes characterized by MS, IR, UV-Vis, fluorescence spectra and thermogravimetric analysis. The cyclic voltammetry tests of C1, C2 and C3 were carried out. It was found that C1 showed the largest redox peaks, while C2 and C3 were not obvious. Therefore, the modified glassy carbon electrode was prepared by electrodeposition using C1 as the electron media for studying behavior of paracetamol (PR) and 4-aminophenol (4-AP) by cyclic voltammetry. The results showed that the oxidation peak (anodic peak) of 4-AP and PR was significantly higher than that of bare glassy carbon electrode. The method had been applied to the simultaneous detection of PR and 4-AP in paracetamol tablets with satisfactory results.

2. EXPERIMENT

2.1. Reagents and materials

O-carboxy benzaldehyde was purchased from Shanghai Maclean Biochemical Technology Co., Ltd. Anhydrous ethanol was purchased from Chengdu Kelong Chemical Reagent Factory. 3-carboxybenzaldehyde, 4-formylbenzoic acid, 2,6-diaminopyridine, cobalt acetate, tetrabutylammonium

perchlorate, acetaminophen and 4-aminophenol were purchased from Aladdin Reagent (Shanghai) Co., Ltd. Acetic acid (36%), glacial acetic acid (99.5%), N,N-dimethylformamide, dimethyl sulfoxide, dichloromethane, chloroform, sodium hydroxide, potassium chloride, sodium acetate, hydrochloric acid, disodium hydrogen phosphate, soluble starch, sodium carbonate, sodium dodecyl sulfate, and sodium dihydrogen phosphate dodecahydrate were purchased from Xiqiao Chemical Industry Co., Ltd. Dextrin was purchased from Guangdong Taishan Chemical Plant. All aqueous solutions were prepared with milli-Q water.

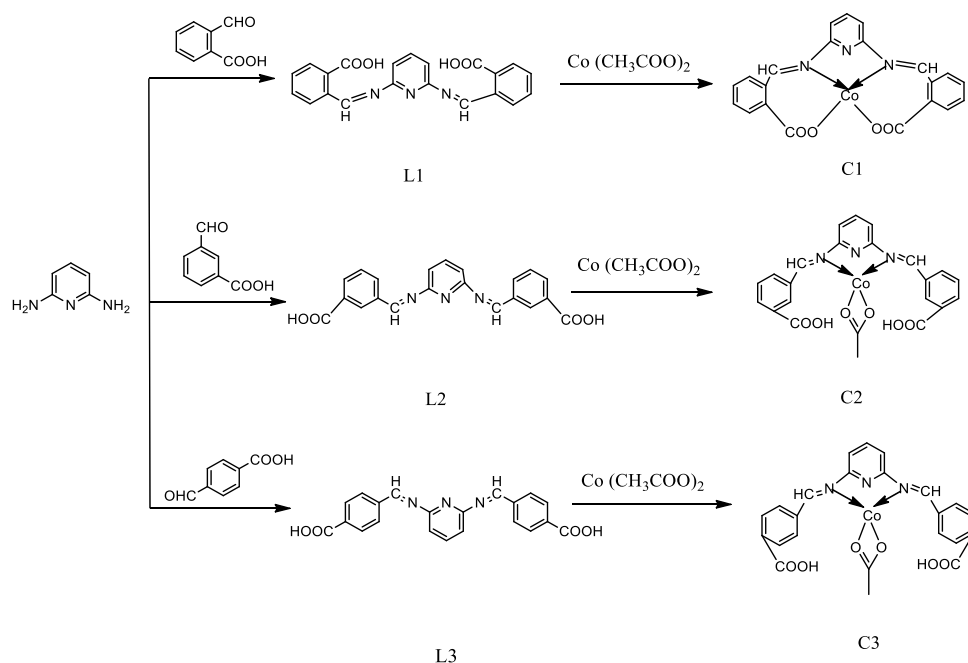
2.2. Apparatus

Mass spectra were measured in an ESI+ mode at 150 V by APEX IV Fourier transform high resolution mass spectrometer of Brooke Dalton Company, USA. The infrared spectrum was measured in a range of 4000 to 400 cm^{-1} by KBr compression by Shimadzu FTIR-8400 Fourier transform infrared spectrometer. UV-Vis spectra were measured by Shimadzu UV-2450 UV spectrometer, test conditions: DMF was used as a reference solution at room temperature, and the sample solution to be tested was $1 \times 10^{-4} \text{ mol} \cdot \text{L}^{-1}$. The F-4600 type Hitachi fluorescence spectrometer of Hitachi Hi-tech Company of Japan was used to measure the fluorescence emission spectrum, test conditions: DMF was used as a reference solution at room temperature, the sample concentration was $1 \times 10^{-4} \text{ mol} \cdot \text{L}^{-1}$, the slit of excitation light and emission light was set to 5 nm, and the scan speed was $1200 \text{ nm} \cdot \text{min}^{-1}$. The thermogravimetric analysis was carried out by using STA-449 thermogravimetric analyzer of Nechi Company in Germany, test conditions: control nitrogen gas flow rate was $100 \text{ mL} \cdot \text{min}^{-1}$, heating rate was $10 \text{ }^\circ\text{C} \cdot \text{min}^{-1}$, temperature range from 25 to 900°C . The surface morphology of the bare glassy carbon electrode and 2,6-diaminopyridine-o-carboxyl benzaldehyde bis-schiff base cobalt complex/glassy carbon electrode were observed by a field emission scan electron microscope manufactured by Japan Hi-Tech Co., Ltd./Oxford, UK. All electrochemical tests were performed by using the CHI 760 electrochemical workstation of Shanghai Chenhua Instruments Co., Ltd. For electrochemical tests, a three-electrode system was used, with a modified glassy carbon electrode as the working electrode, an saturated calomel electrode (SCE) electrode as the reference electrode, and the platinum wire electrode as an auxiliary electrode, the supporting electrolyte was $0.1 \text{ mol} \cdot \text{L}^{-1}$ tetra-n-butylammonium perchlorate (TBAP).

2.3. Synthesis

2.3.1. Preparation of 2,6-Diaminopyridine Double Schiff Bases

2,6-diaminopyridine was used as starting material, which reacts with o-carboxy benzaldehyde, m-carboxy benzaldehyde and p-carboxy benzaldehyde to form 2,6-diaminopyridine-o-carboxyl benzaldehyde bis-schiff base, 2,6-diaminopyridine-m-carboxyl benzaldehyde bis-schiff base and 2,6-diaminopyridine-p-carboxyl benzaldehyde bis-schiff base, noted as L1, L2 and L3 (Scheme 1), respectively.



Scheme 1. Synthetic routes of anions receptors L1, L2 and L3, C1, C2 and C3

2.3.2. Preparation of Cobalt Complexes

L1, L2, and L3 were reacted with cobalt acetate to form 2,6-diaminopyridine-*o*-carboxyl benzaldehyde bis-schiff base cobalt complex, 2,6-diaminopyridine-*m*-carboxyl benzaldehyde bis-schiff base cobalt complex and 2,6-diaminopyridine-*p*-carboxyl benzaldehyde bis-schiff base cobalt complex, noted as C1, C2 and C3 (Scheme 1), respectively.

2.3.3. Preparation of Schiff base cobalt complex modified electrode

(1) Polished glassy carbon electrodes (ϕ is 2 mm) onto the suede to the mirror surface with different sizes of nano-alumina (0.03 and 0.1 μm) powder, sonicated for 20 minutes in distilled water and washed with distilled water. Dry in an oven at 50°C for 5 minutes.

(2) Cyclic voltammetry was used with a three-electrode system that the bare glassy carbon electrode as the working electrode, the Ag/AgCl electrode as the reference electrode, and the platinum wire electrode as the auxiliary electrode, and tetra-*n*-butylammonium perchlorate (TBAP) was added as a supporting electrolyte, the potential range from -1.5 to 1.5 V, the electrodeposition rate was 50 $\text{mV}\cdot\text{s}^{-1}$, and the number of electrodeposition cycles was 20, 0.01 $\text{mol}\cdot\text{L}^{-1}$ C1 in dimethyl sulfoxide (DMSO) was deposited on the surface of the glassy carbon electrode, and the prepared electrode was dried at room temperature for use.

3. RESULTS AND DISCUSSION

3.1. Characterization of Schiff bases and their cobalt complexes

Fig.S1A, B, and C are mass spectra of L1, L2, and L3, respectively. It can be seen from Fig.S1A, B, and C that the molecular ion peaks $[M-COOH-OH+K]^+$ of L1, L2 and L3 all appear at m/z 351.2, which are formed by the loss of the carboxyl and hydroxyl groups and then binding to K^+ [40]. The relative molecular mass of K is 39.1, all of the relative molecular masses of the analytes L1, L2 and L3 are 374.1, indicating that the relative molecular masses of L1, L2 and L3 are consistent with their theoretical relative molecular masses of 373.1. The molecular ion peaks $[M+H]^+$ of L1, appears at m/z 374.1, this is consistent with the relative molecular mass 373.1 of the analyte.

Fig. S2A are the infrared spectrum of L1, L2, and L3. It can be seen from the figure that 771 cm^{-1} is the C-H out-of-plane deformation vibration absorption peak of the benzene ring ortho-substitution of L1, 757 cm^{-1} is the C-H out-of-plane deformation vibration absorption peak of the benzene ring meta-substitution of L2, and 1184 cm^{-1} is the C-H in-plane deformation vibration absorption peak of the benzene ring para-substituted of L3. The carboxyl C-O stretching vibration absorption peaks of the three ligands appeared at 1268 cm^{-1} , 1252 cm^{-1} , and 1266 cm^{-1} , respectively. L1, L2, and L3 did not show stretching vibration absorption peaks in the range of $3390\sim 3170\text{ cm}^{-1}$, indicating that $-NH_2$ does not exist; there are no stretching vibration absorption peak in the range of $1750\sim 1710\text{ cm}^{-1}$, indicating that $-CHO$ is absent. L1, L2, and L3 exhibited C=N stretching vibration absorption peaks at 1646 cm^{-1} , 1647 cm^{-1} , and 1645 cm^{-1} , respectively, indicating the formation of schiff base structure, otherwise, L1 has a carboxyl O-H in-plane deformation vibration absorption peak at 1401 cm^{-1} .

Fig.S2B are the infrared spectrum of C1, C2, and C3. The stretching vibration absorption peak of C1 shifts to 1610 cm^{-1} , and the absorption vibration peak of the carboxyl O-H in-plane shifts to 1381 cm^{-1} , which indicates that C=N and COOH participate in the coordination of metal cobalt ions. A new absorption peak appears at $520\sim 700\text{ cm}^{-1}$, which can be attributed to the stretching vibration absorption peaks of Co-O and Co-N [32,41]. The C=N stretching vibration absorption peaks of C2 and C3 were respectively shifted to 1610 cm^{-1} and 1605 cm^{-1} , indicating that C=N participates in the coordination of metal cobalt ions. C2 and C3 have new absorption peaks at $520\sim 700\text{ cm}^{-1}$, which can be attributed to the stretching vibration peak of Co-N, and new absorption peak appeared at $1422\sim 1458\text{ cm}^{-1}$, which can be attributed to the characteristic absorption peak of acetate in the complex.

As shown in Fig.S3, the absorption peaks of C1, C2, and C3 corresponding to L1, L2, and L3 at 268 nm have undergone a red shift, shifting to 269 nm, 270 nm, and 271 nm, respectively, all of these can be attributed to $\pi-\pi^*$ electron transitions of benzene rings. The absorption peaks of C1 corresponding to L1 at 318 nm have undergone a red shift, shifting to 319 nm, the absorption peaks of C2 corresponding to L2 at 323 nm undergone a red shift, shifting to 333 nm, and the absorption peaks of C3 corresponding to L3 at 322 nm have undergone a red shift, shifting to 323 nm, all of these can be attributed to $n-\pi^*$ electronic transitions with benzene ring conjugated C=N [41]. The reason for the red shift may be due to the transfer of electrons from the ligand to the metal ion (LMCT) during the molecule [6]. The new absorption peak of the cobalt complex C1 at 398 nm may be due to the d-d transition inside the Co(III) octahedral field [41].

As shown in Fig.S4, L1, L2, L3 have their fluorescent properties, which is due to the existence of large conjugated π bonds in the schiff-base structure that easy emission fluorescence. The maximum excitation wavelengths of L1, L2, and L3 were 318, 323, and 322 nm, and the emission wavelengths were 370, 375, and 374 nm, respectively. The maximum excitation wavelengths of cobalt complexes C1, C2, and C3 were 318, 270, and 271 nm, and the emission wavelengths were 456, 362, and 347 nm, respectively.

Compared with the ligand L1, the cobalt complex C1 undergoes a red shift at the emission wavelength and moved from 370 nm to 456 nm, because the coordination of the ligand increases the conjugated structure, and the energy loss due to vibration and rotation of the excited molecule decreases, resulting in total energy, the system is reduced and red shift occur[42]. Compared with the ligands L2 and L3, the cobalt complexes C2 and C3 exhibit blue shift at different degrees, the cobalt complex C2 undergoes a blue shift at the emission wavelength and moved from 375 nm to 362 nm, the cobalt complex C3 undergoes a blue shift at the emission wavelength and moved from 374 nm to 347 nm. It may be due to the coordination of the ligands with the metal ions, resulting in an increase in the HOMO-LUMO energy level difference[43]. The fluorescent intensity of the cobalt complexes C1, C2, and C3 were lower than that of the ligands L1, L2, and L3, it may be after the formation of cobalt complex, the center ion cobalt ion has paramagnetism, and there is a jump between the first excited singlet (S1) and the first excited triplet (T1), which leads to the loss of fluorescence energy and the decrease of fluorescent intensity. The fluorescence intensity of these six compounds follows the order of $L1 > L3 > L2$, $C3 > C2 > C1$.

As can be seen from Fig.S5A, the weight loss rate of L1 before 77°C is only 2.7%, which is due to the decomposition of residual solvent (anhydrous ethanol) in the double Schiff base, then the thermogravimetric curve continues to decline, and L1 gradually decomposes. When the temperature reaches 180°C, the skeleton collapses, and the final residual amount is about 48.3%, which may be due to the carbon deposition effect caused by the high carbon content of L1 [44]. It can be seen from Fig.S5C that before 320°C, the thermogravimetric curve of L2 is a platform, indicating that the double schiff base does not decompose; as the temperature increases, the thermogravimetric curve drops sharply, and the skeleton of L2 gradually collapsed, the final residual amount is 19.8%, which may be due to the carbon deposition effect caused by the high carbon content of L2. Similarly, as can be seen from Fig.S5E, before 185°C, the thermogravimetric curve of L3 is a platform, indicating that the double schiff base does not decompose; As the temperature rises, the thermogravimetric curve drops sharply, and L3 begins to decompose gradually, the skeleton collapsed, and the final residual amount is about 9.3%, which may be due to the carbon deposition effect caused by the high carbon content of L3. Comparing these three substances, the order of thermal stability is $L2 > L3 > L1$.

As can be seen from Fig.S5B, with the temperature increases, the thermogravimetric curve of C1 falls, and the weight loss rate before 103°C is 4.2%, which is caused by the decomposition of the solvent (water) remaining in the complex C1. The temperature continues to rise, and C1 begins to decompose gradually. When the temperature reaches 349 °C, the skeleton begins to collapse, and the final residual amount is about 16.3%, the residual material should be Co_2O_3 [45].It can be seen from Fig.S5D that before 70°C, the thermogravimetric curve of C2 is a platform, indicating that the double schiff base did not decompose, as the temperature increases, the thermogravimetric curve declines and the complex C2

begins to decompose until the skeleton collapses. The final residual amount is about 11.8%, and the residual material should be Co_2O_3 . It can be seen from Fig.S5F that before 78°C , the thermogravimetric curve of C3 is a platform, indicating that the complex does not decompose; As the temperature increases, the thermogravimetric curve declines and the skeleton of complex C3 begins to collapse. The final residual amount is about 35.1%, and the residual material should be Co_2O_3 . Comparing the thermal stability of three Schiff base transition metal complexes, the order of thermal stability is $\text{C1} > \text{C2} > \text{C3}$.

3.2. Cyclic Voltammetric Characteristics of bis-schiff base cobalt complexes

It can be seen from Fig.1 that C1 exhibits a pair of obvious redox peaks, which oxidation peak appeared near -0.8 V , the peak current was $-108\ \mu\text{A}$, the reduction peak appeared near -0.7 V , and the peak current was $54\ \mu\text{A}$, it was indicated that a quasi-reversible redox reaction occurs in C1, which was attributed to electron transfer of oxidation-reduction pair of Co(III)/Co(II) . However, the redox peaks of C2 and C3 were not obvious, the cyclic voltammetry behavior of the three cobalt complexes were different, which may be due to the difference between the position of carboxyl group in bis-Schiff base and the coordination mode of Co(II) .

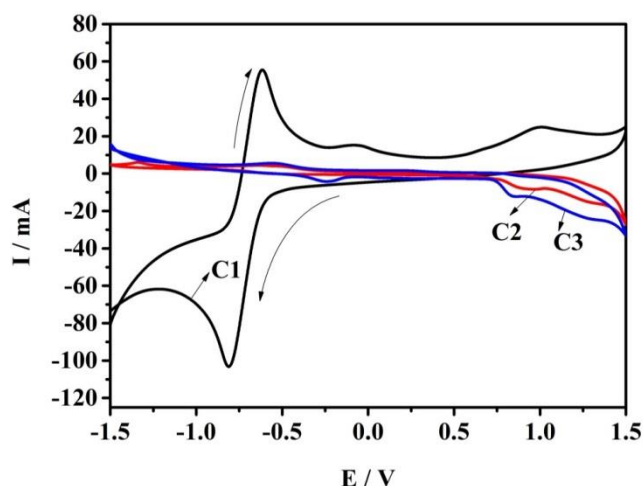


Figure 1. The CV curves of C1, C2 and C3 (The test conditions: the solvent was dimethyl sulfoxide (DMSO), support electrolyte was $0.1\ \text{mol}\cdot\text{L}^{-1}$ tetra-n-butylammonium perchlorate (TBAP), potential range from -1.5 to 1.5 V , and scan rate was $50\ \text{mV}\cdot\text{s}^{-1}$)

The smaller the peak potential difference, the larger the peak current and the better the electrochemical performance [46]. The redox peak potentials difference of C1, C2, and C3 are 0.19 , 0.11 and 0.33 V as calculated from Figure 1, respectively. The peak potential difference between C1 and C2 is similar, and the peak current C1 is much larger than C2, therefore, C1 was selected as modified electrode.

The surface morphology of the bare glassy carbon electrode and the modified electrode were examined by a S-4800 field emission scan electron microscope. The results were shown in Fig.2. The surface of the pre-treated glassy carbon electrode (Fig.2A) is smooth, while the surface of the modified

electrode (Fig.2B) has irregular granular substance, which further proves that the bis-Schiff base cobalt complex has been electrodeposited on the glassy carbon electrode surface.

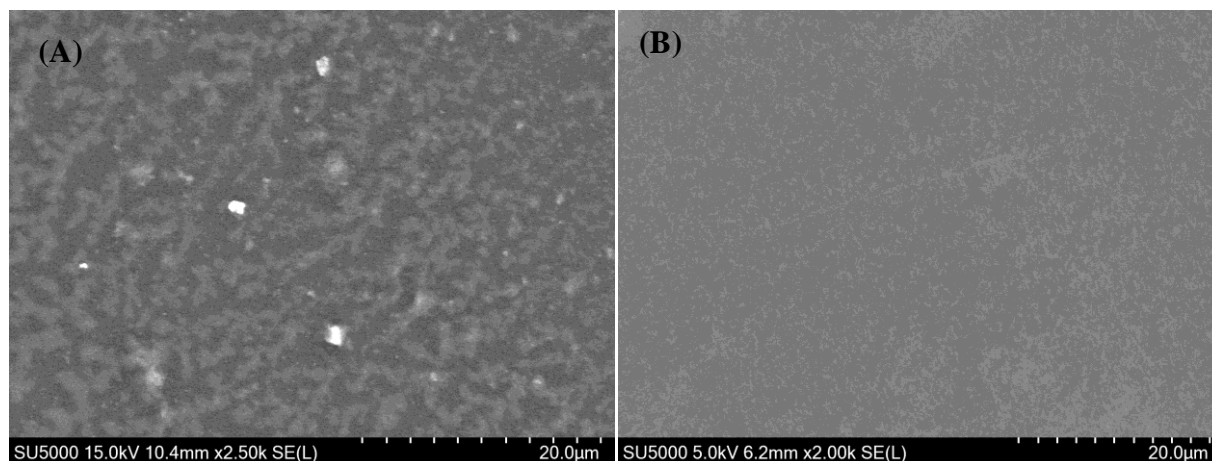


Figure 2. Scan electron microscopy of different glassy carbon electrodes (A. Bare glassy carbon electrode; B. C1 modified electrode)

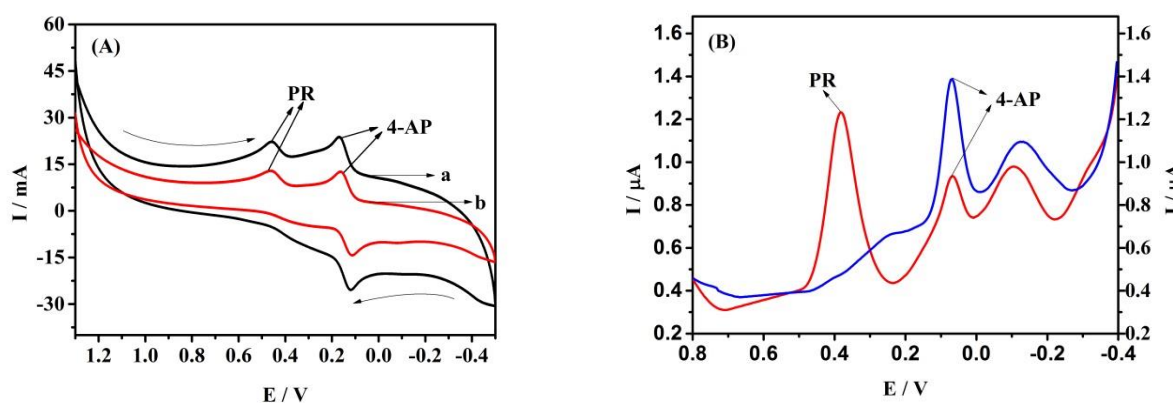


Figure 3. (A) CV curves of PR and 4-AP on different electrodes (a. Modified electrode; b. Bare GCE)(At $50 \text{ mV}\cdot\text{s}^{-1}$, the cyclic voltammograms of $0.1 \text{ mmol}\cdot\text{L}^{-1}$ PR and 4-AP were detected simultaneously in $0.1 \text{ mol}\cdot\text{L}^{-1}$ PBS solution (pH 7); (B) DPV curves of PR and 4-AP on modified glassy carbon electrode($5 \text{ }\mu\text{mol}\cdot\text{L}^{-1}$ PR and $5 \text{ }\mu\text{mol}\cdot\text{L}^{-1}$ 4-AP were detected simultaneously in $0.1 \text{ mol}\cdot\text{L}^{-1}$ PBS solution (pH 7)

Fig.3A and B shows a CV and DPV when the electrodeposition rate was $50 \text{ mV}\cdot\text{s}^{-1}$, $0.1 \text{ mmol}\cdot\text{L}^{-1}$ PR and 4- AP are simultaneously detected in a $0.1 \text{ mol}\cdot\text{L}^{-1}$ PBS solution (pH = 7) by using bare glassy carbon electrode and modified electrode, respectively.

As shown in Fig.3A, the anode peak of the modified electrode is higher than that of the bare glassy carbon electrode, indicating that the PR and 4-AP have a fast electron transfer process at the modified electrode. It may be due to the presence of cobalt complexes with various oxidation states and good electrochemical redox properties on the surface of the modified electrode [47]. In addition, there are two anodic peaks and one cathodic peak in the curve, which indicates that there are different electrode reaction processes. The electrode reaction process of PR on the modified glassy carbon electrode is

irreversible and the electrode reaction process of 4-AP on the modified glassy carbon electrode is a quasi-reversible. Before the modification, the oxidation peak potential of PR was 0.46 V, the peak current was 14.5 μA , the oxidation peak potential of 4-AP was 0.16 V, and the peak current was 14.7 μA . After modification, the oxidation peak potential of PR was 0.46 V, the peak current was 22.5 μA , the oxidation peak potential of 4-AP was 0.16 V, and the peak current was 23.3 μA . The oxidation peak separation of modified electrode was more obvious than that of bare glassy carbon electrode. The peak potential difference between the two electrodes was 0.30 V, and the peak current was higher than that of bare glassy carbon electrode, it shows the rapid electron transfer process of PR and 4-AP on the modified electrode. The voltammetric response of PR and 4-AP is greatly improved on the glassy carbon electrode modified by the double schiff base cobalt complex. The separation of the two oxidation peaks on the modified electrode is significant enough to detect both PR and 4-AP. The modified electrode has two peaks and enhanced peak current, exhibits good electrocatalytic activity, and has high selectivity and sensitivity for simultaneous detection of PR and 4-AP.

From Fig.3B, two oxidation peaks appear in the curve, the peak shape is sharp and the peak current is large, the oxidation peak of 0.38V belongs to PR, the peak current was 0.64 μA , the oxidation peak of 0.07 V belongs to 4-AP, the peak current was 1.12 μA , the results show that the oxidation peak of the modified glassy carbon electrode is well separated, and the potential difference between PR and 4-AP is 0.31 V, indicating that the modified electrode has a strong catalytic effect on PR and 4-AP, and the sensitivity is high, which can be used for simultaneous detection of PR and 4-AP.

3.3. Optimization of preparation conditions and detection

(1) Effect of electrode deposit circulation of C1

According to the method shown in 2.3.3, changing the number of electrodeposition cycles (15, 18, 20, 22 and 25 turns), and prepare five cobalt complex modified electrodes.

As shown in Fig.S6, the current of the oxidation peak gradually increases with the increase of the number of electrodeposition cycles. When 20 cycles of electrodeposition, the peak current reaches a maximum value, and then as the number of electrodeposition cycles increases, the peak current decreases. This is because with the increase of the number of electrodeposition cycles, C1 is continuously deposited on the surface of the glassy carbon electrode, increases the surface area of the electrode and promotes electron transfer, resulting in a gradual increase in the oxidation peak current. The current of the oxidation peak decreases gradually after the number of electrodeposition cycles reaches 20 laps, which may be due to the large thickness of the complex film, the larger resistance of electron movement in the film, and the decrease of the transfer rate, which leads to the decrease of the current. Therefore, the optimal electrodeposition number of the modified electrode prepared in this paper is 20.

(2) Effect of electrodeposition rate of C1

According to the method shown in 2.3.3, the electrodeposition rate was changed (50, 100, 150, 200 and 250 $\text{mV}\cdot\text{s}^{-1}$), and five cobalt complex modified electrodes were prepared.

As shown in Fig.S7, the peak current was maximum at the electrodeposition rate of 50 $\text{mV}\cdot\text{s}^{-1}$. The current of the oxidation peak decreases with the increase of the electrodeposition rate. After that, as

the electrodeposition rate continues to increase, the oxidation peak current gradually decreases. This is because the electrodeposition rate affects the shape and thickness of the cobalt complex film. When the electrodeposition rate is too large, the thickness of the cobalt complex becomes large and rough, resulting in a decrease in the peak current. When the electrodeposition rate is less than $50 \text{ mV}\cdot\text{s}^{-1}$, it takes a long time to deposit cobalt complex on glassy carbon electrode with the same thickness. Thus it can be obtained that the best electrodeposition rate was $50 \text{ mV}\cdot\text{s}^{-1}$.

(3) Effect of pH values

In general, the involvement of protons is involved in the electrochemical process. Therefore, different pH values of phosphate buffer solution (PBS) affect the electrochemical process of PR and 4-AP [49,50]. The three-electrode system was used to study the electrochemical behavior of the cobalt complex modified electrode that in different pH PBS buffer solution, the simultaneous detection concentration is $0.1 \text{ mmol}\cdot\text{L}^{-1}$ PR and 4-AP. The results are shown in Fig.S8. Test conditions: The voltage range from -0.5 to 1.3 V, the scan rate is $50 \text{ mV}\cdot\text{s}^{-1}$, change the pH of the PBS buffer solution from 5 to 9 for the experiment.

As shown in Fig.S8, with the increase of pH, the peak potential moves negatively and the oxidation peak current increases. When $\text{pH}=7$, the peak current was the highest for the detection of PR and 4-AP, the separation of the two anodic peaks was obvious, and there was a good electrochemical response. This may be because in the acidic medium, high concentration of H^+ can react with PR and 4-AP, which will reduce the adsorption amount of cobalt complex on the surface of the electrode, similarly, high concentrations of OH^- will also reduce the amount of cobalt complexes adsorbed, so the peak current becomes lower than at neutral pH ($\text{pH} = 7$) [47]. Therefore, the optimum pH condition for simultaneous determination of PR and 4-AP at cobalt modified electrode was $\text{pH} = 7$. According to the relationship between potential and pH, the relationship between the oxidation peak potential of PR and 4-AP and pH is shown in Fig.S8 insert (a) and (b), respectively. The relationship between the reduction peak potential and pH is shown in Fig. S8 insert (c). The equation for PR can be expressed as $E_{\text{pa}}(\text{V}) = 0.81802 - 0.05265 \text{ pH}$, ($R^2 = 0.98605$), and the equation for 4-AP can be expressed as $E_{\text{pa}}(\text{V}) = 0.57636 - 0.06146 \text{ pH}$, ($R^2 = 0.989$), the relationship between the reduction peak potential and pH of the two can be expressed as $E_{\text{pc}}(\text{V}) = -0.4351 + 0.05224 \text{ pH}$, ($R^2 = 0.989$), the above expression clearly demonstrates that protons are directly involved in the electrochemical redox process. According to the relationship between the oxidation peak potential of PR and 4-AP and pH and the following formula, m/n can be calculated.

$$dE_p/d\text{pH} = 2.303mRT/nF,$$

Where m is the number of protons and n is the number of electrons[48]. When the redox reaction occurs in PR, m/n is 0.89 and 0.88, respectively. When the 4-AP undergoes redox reaction, m/n is 1.04 and 0.88, respectively, which indicates that during the electrochemical redox process of PR and 4-AP, the number of protons and electrons is equal. In addition, the change of PR and 4-AP oxidation peak current with pH is shown in Fig. S9 (a) and (b), and the reduction peak current of the two changes with pH is shown in Fig. S9(c).

(4) Effect of different scan rates

The electrochemical behavior of C1 modified electrode for simultaneous test $0.1 \text{ mmol}\cdot\text{L}^{-1}$ PR and 4-AP at different scan rates were studied. The results were shown in Fig.S10. Test conditions: the

voltage range from -0.5 to 1.3 V, the pH of the PBS buffer solution was 7, and change the scan rate 25, 50, 100, 150, 200 and 250 $\text{mV}\cdot\text{s}^{-1}$ for experiments.

As shown in Fig.S10, keeping the other conditions constant, with the scan rate increasing, the oxidation reduction peak potentials of PR and 4-AP are almost unchanged, the oxidation reduction peak current of both PR and 4-AP increase, moreover, the oxidation peak potential moves in a positive direction, and the reduction peak potential moves in a negative direction, it indicates that the redox reversibility of PR and 4-AP got worse.

Taking the square root of the scan rate as the transverse coordinate and the current value of the anodic peak as the vertical coordinate (Fig.S10 insert a), it can be seen that the oxidation peak current of the PR increases with the increase of the scan rate, and the oxidation peak current is proportional to the square root of the scan rate. The linear equation is $I_{pa} = 1.6350v^{1/2} - 2.2108$ (R^2 is 0.99775) and the slope was 1.6350, indicating that the electron transfer process is controlled by diffusion. It can also be seen from Fig.S10 insert b that the oxidation peak current of 4-AP increases with the increase of the scan rate, the oxidation peak current is proportional to the square root of the scan rate. The linear equation is $I_{pa} = 1.8383 v^{1/2} - 3.6405$ (R^2 is 0.99691), with a slope of 1.8383, indicates that the electron transfer process is controlled by diffusion [47]. When the scan rate is too large, the current is too large and the baseline is unstable. At a scan rate of 100 $\text{mV}\cdot\text{s}^{-1}$, the peak shape is stable, so the best scan rate is 100 $\text{mV}\cdot\text{s}^{-1}$.

3.4. Analytical determination of PR and 4-AP

Finally, DPV was used for simultaneous detection of PR and 4-AP. Because DPV is a more sensitive technology than CV, it can eliminate the influence of background current. The range of differential pulse voltammetry was -0.4 ~ 0.8 V, the increment is 0.004 V, the amplitude was 0.025 V, the pulse width was 0.05 s, 0.1 $\text{mol}\cdot\text{L}^{-1}$ sodium hydrogen phosphate and 0.1 $\text{mol}\cdot\text{L}^{-1}$ sodium dihydrogen phosphate (pH 7) are used as buffer solution.

3.4.1. DPV diagram of PR and 4-AP with different concentration

Keeping the 4-AP concentration constant at 1 $\mu\text{mol}\cdot\text{L}^{-1}$, and change the concentration of PR at 5 $\mu\text{mol}\cdot\text{L}^{-1}$, 10 $\mu\text{mol}\cdot\text{L}^{-1}$, 15 $\mu\text{mol}\cdot\text{L}^{-1}$, 20 $\mu\text{mol}\cdot\text{L}^{-1}$ and 30 $\mu\text{mol}\cdot\text{L}^{-1}$, in a PBS solution at pH=7, differential pulse voltammetric behavior of bis-Schiff base cobalt complex modified electrode was studied. According to Fig.4, the oxidation peak current of PR increases with the increase of PR concentration. The concentration of PR was used as the coordinate and the current value of the anode peak was drawn in the vertical coordinate, the result was shown in Fig.4 insert(a), we can see that the oxidation peak current of PR has a good linear relationship with its concentration in the concentration range from 5 to 30 $\mu\text{mol}\cdot\text{L}^{-1}$. The linear equation was $I_{pa} = 0.034 C + 0.536$ (R^2 is 0.9904), the slope was 0.034, the noise-signal ratio was 3, the detection limit was 1.86 $\mu\text{mol}\cdot\text{L}^{-1}$ [49].

Keeping the PR concentration constant at 1 $\mu\text{mol}\cdot\text{L}^{-1}$, and change the concentration of 4-AP at 5 $\mu\text{mol}\cdot\text{L}^{-1}$, 10 $\mu\text{mol}\cdot\text{L}^{-1}$, 15 $\mu\text{mol}\cdot\text{L}^{-1}$, 20 $\mu\text{mol}\cdot\text{L}^{-1}$ and 30 $\mu\text{mol}\cdot\text{L}^{-1}$, in a PBS solution at pH=7, differential

pulse voltammetric behavior of bis-schiff base cobalt complex modified electrode was studied. According to Fig.4, the oxidation peak current of 4-AP increases with the increase of 4-AP concentration. The concentration of 4-AP was used as the coordinate and the current value of the anode peak was drawn in the vertical coordinate, the result was shown in Fig.4 insert(b), we can see that the oxidation peak current of 4-AP has a good linear relationship with its concentration in the concentration range from 5 to 30 $\mu\text{mol}\cdot\text{L}^{-1}$. The linear equation was $I_{\text{pa}} = 0.02462C + 1.03693$ (R^2 is 0.9929), the slope was 0.02462, the noise-signal ratio was 3, the detection limit was 2.08 $\mu\text{mol}\cdot\text{L}^{-1}$ [51-53].

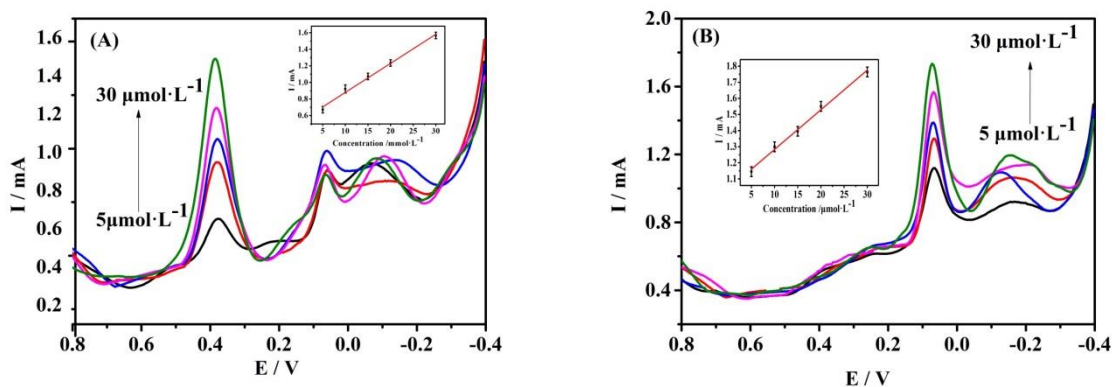


Figure 4. DPV diagram of oxidation peak current of PR (A) and 4-AP (B) at different concentrations. The test conditions: voltage range from -0.4 to 0.8 V, increment was 0.004 V, amplitude was 0.025 V, pulse width was 0.05 s, buffer solution was 0.1 $\text{mol}\cdot\text{L}^{-1}$ disodium hydrogen phosphate and sodium dihydrogen phosphate solution (pH 7). (A) keep the 4-AP concentration constant at 1 $\mu\text{mol}\cdot\text{L}^{-1}$, and change the concentration of PR at 5 $\mu\text{mol}\cdot\text{L}^{-1}$, 10 $\mu\text{mol}\cdot\text{L}^{-1}$, 15 $\mu\text{mol}\cdot\text{L}^{-1}$, 20 $\mu\text{mol}\cdot\text{L}^{-1}$ and 30 $\mu\text{mol}\cdot\text{L}^{-1}$, differential pulse voltammetry behavior of Schiff base cobalt complex modified glassy carbon electrode in PBS solution with pH=7 was investigated. (From inside to outside 4-AP were 5, 10, 15, 20 and 30 $\mu\text{mol}\cdot\text{L}^{-1}$, the insert was a graph of the oxidation peak current of PR at different concentrations as a function of concentration.) (B) keep the PR concentration constant at 1 $\mu\text{mol}\cdot\text{L}^{-1}$, and change the concentration of 4-AP at 5 $\mu\text{mol}\cdot\text{L}^{-1}$, 10 $\mu\text{mol}\cdot\text{L}^{-1}$, 15 $\mu\text{mol}\cdot\text{L}^{-1}$, 20 $\mu\text{mol}\cdot\text{L}^{-1}$ and 30 $\mu\text{mol}\cdot\text{L}^{-1}$, differential pulse voltammetry behavior of Schiff base cobalt complex modified glassy carbon electrode in PBS solution with pH=7 was investigated. (From inside to outside PR were 5, 10, 15, 20 and 30 $\mu\text{mol}\cdot\text{L}^{-1}$, the insert was a graph of the oxidation peak current of 4-AP at different concentrations.)

Table 1 lists the simultaneous detection of acetaminophen and 4-aminophenol by different chemically modified electrodes. It can be seen from the table. It can be seen from the table that the chemically modified electrode used in this experiment simultaneously detects PR and 4-AP, and has a relatively low detection limit (PR for 1.86 μM , 2.08 μM for 4-AP), indicating that the double Schiff base cobalt complex modified by this experiment has relatively high sensitivity to PR and 4-AP, the double Schiff base cobalt complex modified electrode is expected to be applied to detect other substances.

Table 1. Comparison of chemically modified electrodes for simultaneous detection of Acetaminophen and 4-aminophenol

Electrode material	Analyte	Detection Limit	Linear range	Correlation	References
Palladium-Reduced Graphene Oxide with Gold Nanoparticles	Acetaminophen, 4-aminophenol	0.30 μM , 0.12 μM	1-250 μM , 1-300 μM	0.9957, 0.9962	[4]
Droplet-based Microfluidics	4-aminophenol	15.68 μM	50-500 μM	0.9972	[17]
Gold Nanoparticles (AuNPs) and a Layered Double Hydroxide Sodium	Acetaminophen, 4-aminophenol	0.13 μM	0.5-400 μM	0.9972, 0.9973	[22]
CdSe Microspheres	Acetaminophen, 4-aminophenol	0.1 μM	0.5-800 μM	0.9993, 0.9958	[23]
paper-based microfluidic device	Acetaminophen, 4-aminophenol	25.0 μM , 10.0 μM	0.05-2.0 mM	0.999, 0.999	[24]
Poly(Patton and Reeder's) reagent	Acetaminophen	0.53 μM	0.7-100 μM	0.9941	[25]
Bis-schiff Base Cobalt Complexes	Acetaminophen, 4-aminophenol	1.86 μM , 2.08 μM	5-30 μM	0.9904, 0.9929	this work

3.4.2. Stability of modified electrode

The modified electrode was prepared and subjected to CV. Test conditions: The potential range from -1.5 to 1.5 V, the scan rate was $50 \text{ mV}\cdot\text{s}^{-1}$, and the number of scan circle was 20. The test result is shown in Fig.S11.

Fig.S11 showed that the CV curves become more stable with the increase of the number of scan cycles during the scan process, indicating that cobalt complexes have been electrodeposited on the surface of glassy carbon electrodes. A pair of obvious redox peaks appear in Fig.S11, the peak potential of the oxidation peak was -0.58 V, and the peak potential of the reduction peak was -0.88 V. which can be attributed to the electron transfer of Co(III)/Co(II) redox electric pair with a potential difference of 0.29 V, it showed that the electrode reaction process has poor reversibility.

The prepared cobalt complex modified electrode was placed at room temperature, placed in the air for a week, under the optimal detection conditions of the voltage range from -0.5 to 1.3 V and the scan rate of $100 \text{ mV}\cdot\text{s}^{-1}$, the PR and 4-AP solutions were measured 5 times in parallel by CV, and the peak current of oxidation peak was not significantly changed (less than 5%). It indicates that the electrode has good stability.

3.4.3. Interference studies

In this test, the control error range was within $\pm 5\%$ under optimal detection conditions, some inorganic ions and organic compounds commonly found in paracetamol were investigated and the effects of $10\ \mu\text{mol}\cdot\text{L}^{-1}$ PR and 4-AP solutions were determined simultaneously. The results were shown in Table S1. From Table S1, we can see that the common excipients in the drug do not interfere with the simultaneous determination of PR and 4-AP.

3.5. Actual sample analysis

10 mL paracetamol tablets (0.3 g PR/tablets) were first prepared and tested by DPV for 5 times. The results are shown in Table S2. The relative standard deviation (RSDs) was 4.92%, which indicates that the method has high precision. 10 mL tablet solution, $15\ \mu\text{mol}\cdot\text{L}^{-1}$ PR and $25\ \mu\text{mol}\cdot\text{L}^{-1}$ 4-AP solution were reconfigured and added to 10 mL tablet solution to perform a standard recovery test, the results were shown in Table S2. The recovery rate of PR was 98.7%~101.2%, and the recovery rate of 4-AP was 98.4%~101.6%. The recovery test shows that the method has high accuracy. The cobalt complex modified electrode developed was feasible for simultaneous determination of PR and 4-AP in drugs.

4. CONCLUSION

In conclusion, the 2,6-diaminopyridine-based bis-Schiff bases and their cobalt complexes were synthesized which have certain fluorescence and thermal stability, and used for modification of electrode, the as-prepared electrode was carried out for PR and 4-AP simultaneous detection in the tablets. The method is simple and low-cost, showing high sensitivity and high recovery rate for PR and 4-AP in tablets. The results demonstrated that the prepared chemically modified electrode can be used for the detection of PR and 4-AP in actual drug samples, and the precision and accuracy of the method are satisfied.

ACKNOWLEDGMENT

This work was supported by the National Nature Science Foundation of China (No. 21266006, 61661014, 61627807), the Nature Science Foundation of Guangxi Province (No. No. 2018GXNSFAA281198, 2018GXNSFBA281135) and Guangxi Key Laboratory of Electrochemical and Magneto-chemical Functional Materials, Collaborative Innovation Center for Exploration of Hidden Nonferrous Metal Deposits and Development of New Materials in Guangxi. This research was supported by the special funding for distinguished expert from Guangxi Zhuang Autonomous Region and Guangxi Colleges and Universities Training Program for 1,000 Middle and Young Cadre Teachers.

SUPPORTING MATERIAL

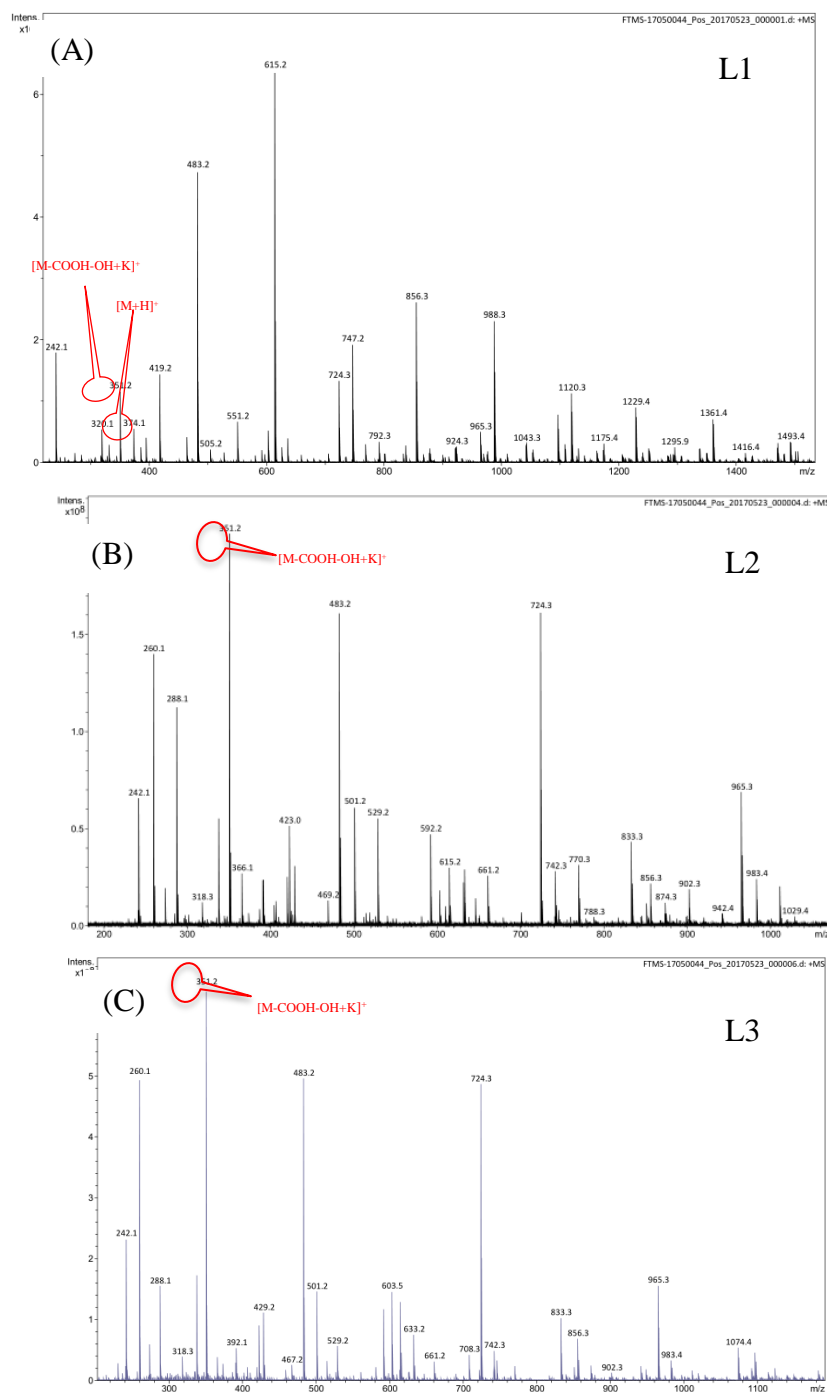


Figure S1. The mass spectrogram of Schiff base compounds L1, L2 and L3

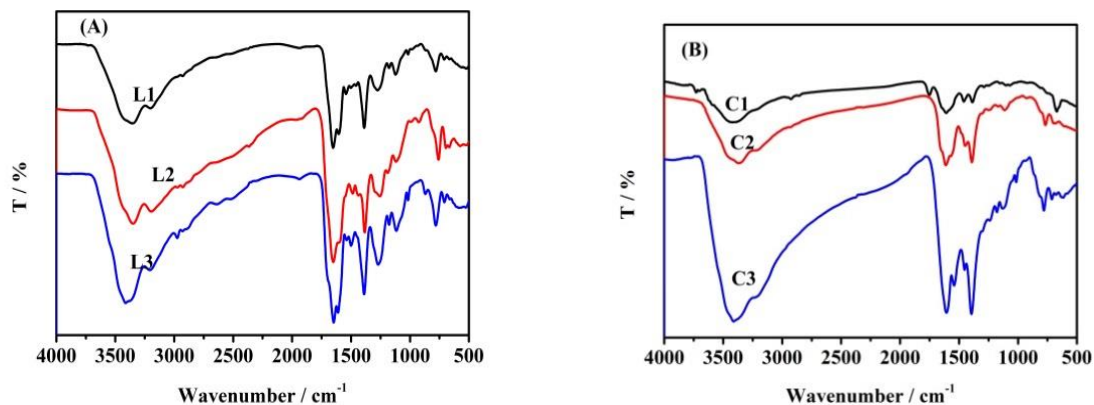


Figure S2. Infrared spectra of Schiff base L1, L2 and L3 (A) and their metal complexes C1, C2 and C3 (B)

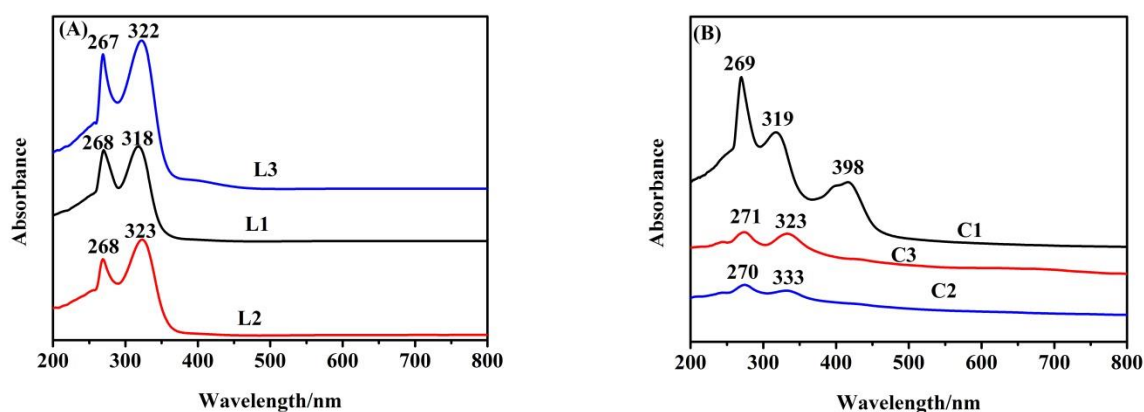


Figure S3. The UV-Vis spectra of Schiff base L1, L2 and L3(A) and their metal complexes (C1, C2 and C3(B); DMF or H₂O as reference solution, the concentration of sample solution was $1.0 \times 10^{-5} \text{ mol} \cdot \text{L}^{-1}$.

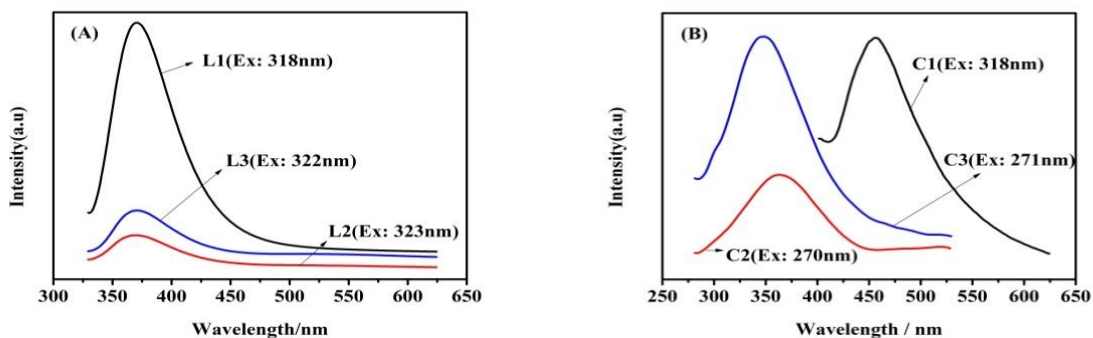


Figure S4. Fluorescence spectra of Schiff base L1, L2 and L3 (A) and their metal complexes C1, C2 and C3 (B); DMF or H₂O as reference solution, the concentration of sample solution was $1.0 \times 10^{-5} \text{ mol} \cdot \text{L}^{-1}$.

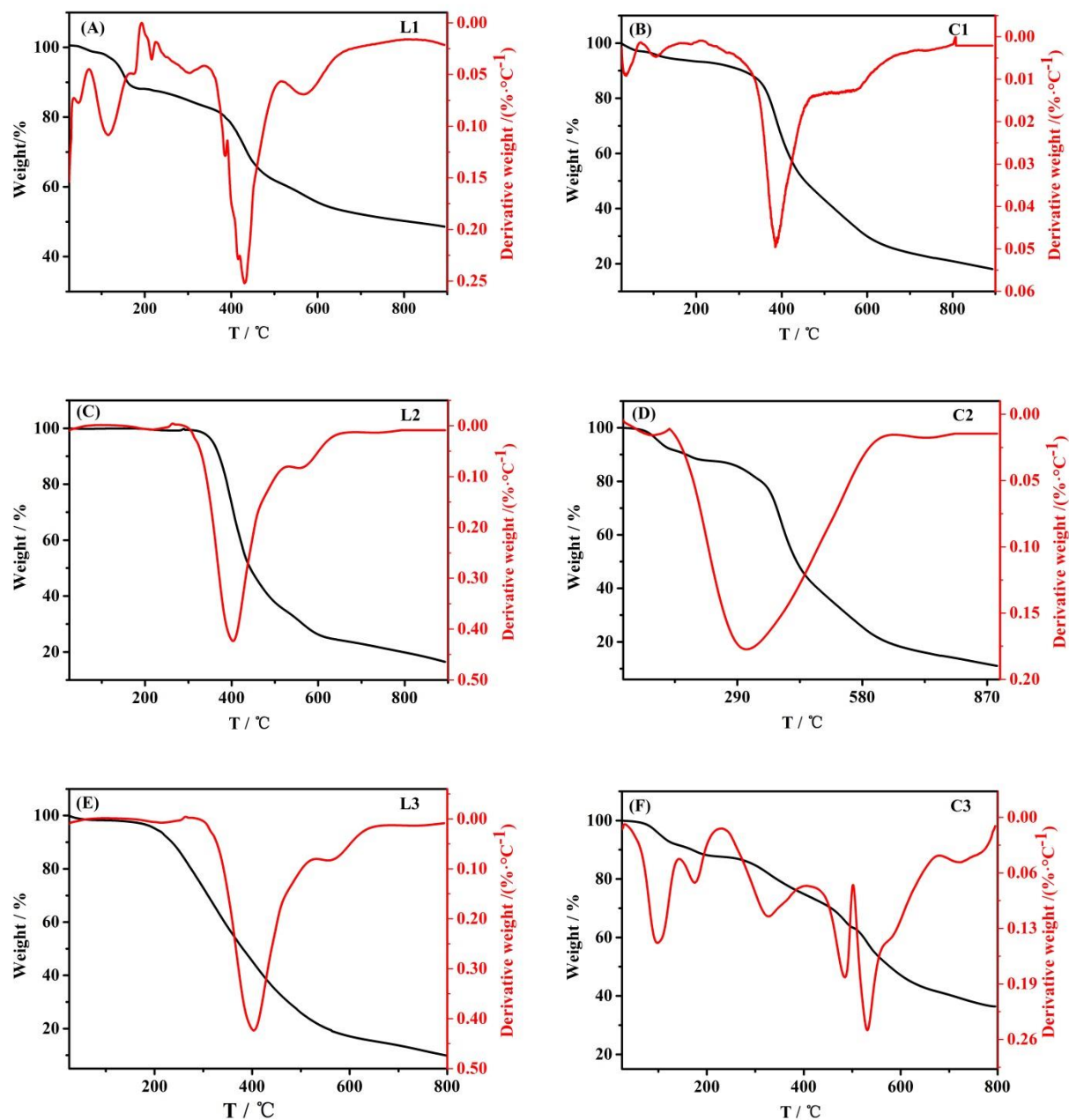


Figure S5. Thermogravimetric curves of Schiff base (L1, L2, L3) and their metal complexes (C1, C2, C3)

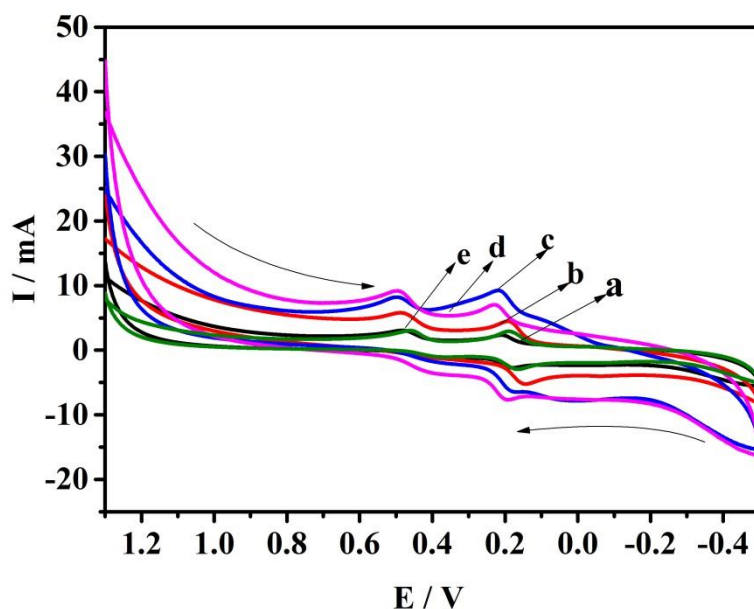


Figure S6. Cyclic voltammograms measured simultaneously under different number of electrodeposition circles; the electrochemical behavior of cobalt complex modified glassy carbon electrode was studied by using C1 modified glassy carbon electrode as a working electrode, Ag/AgCl electrode as a reference electrode and platinum wire electrode as a auxiliary electrode. Test conditions: electrodeposition rate was $50 \text{ mV}\cdot\text{s}^{-1}$, scan rate was $100 \text{ mV}\cdot\text{s}^{-1}$, potential range from -0.5 to 1.3 V. (a→ e: 15, 18, 20, 22, 25 circles)

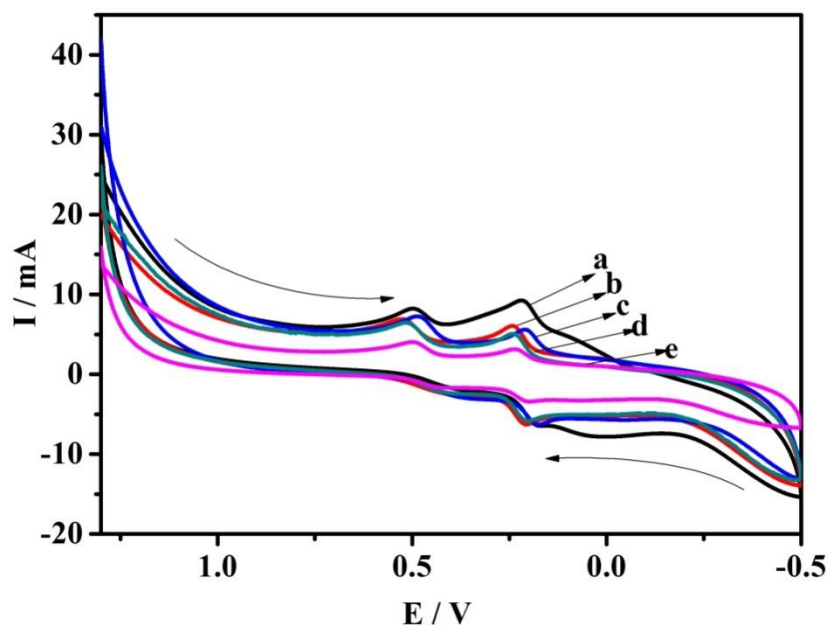


Figure S7. Cyclic voltammograms simultaneously measured at different electrodeposition rates. Test conditions: potential range from -0.5 to 1.3 V, scan rate was $100 \text{ mV}\cdot\text{s}^{-1}$. (a→e: 50, 100, 150, 200, 250 $\text{mV}\cdot\text{s}^{-1}$)

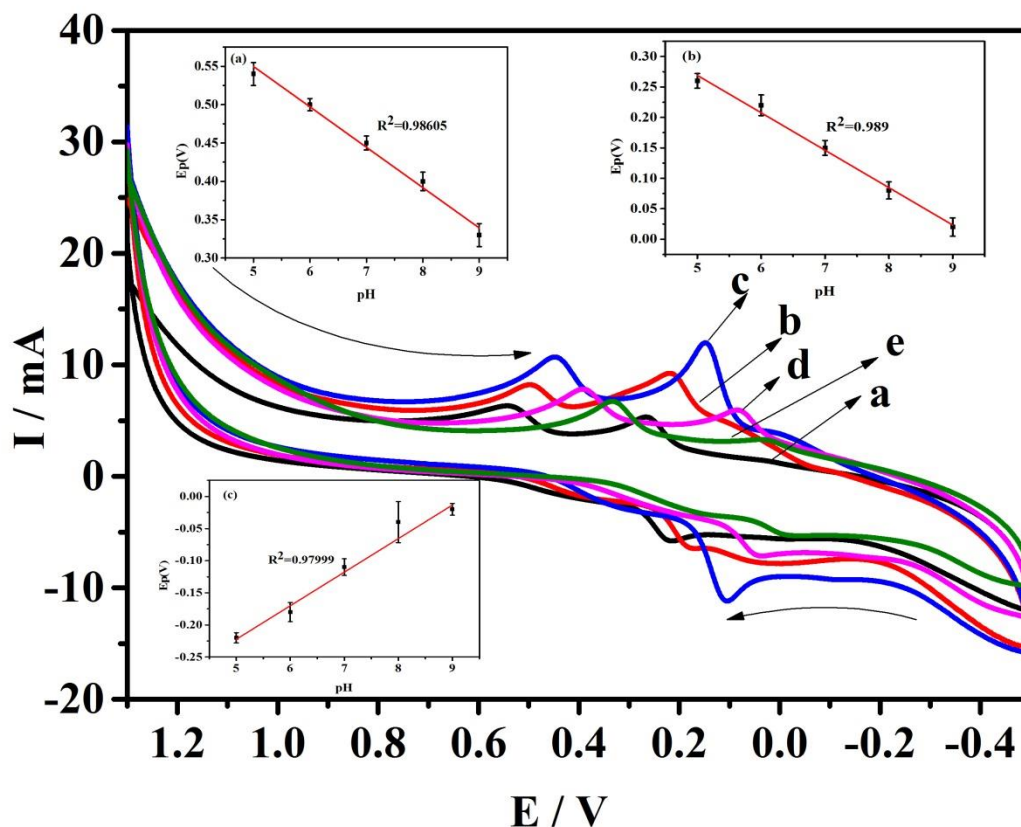
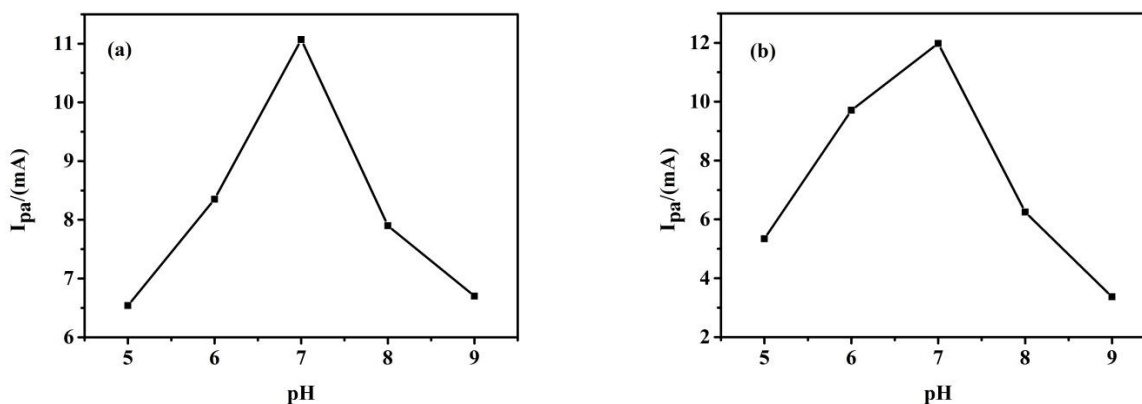


Figure S8. Cyclic voltammograms of modified electrodes in PBS buffers with different pH. Test conditions: potential range from -0.5 to 1.3 V, scan rate was 50 mV s^{-1} , pH value a→e: pH 5, 6, 7, 8, 9. The insert (a) is the effect of pH on the oxidation peak of PR, the insert (b) is the effect of pH on the oxidation peak of 4-AP, and the insert (c) is the effect of pH on the reduction peak current of PR and 4-AP.



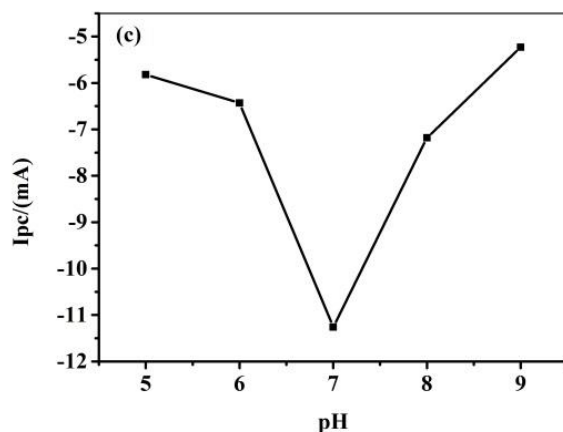


Figure S9: (a) The effect of pH on the oxidation peak current of PR; (b) The effect of pH on the oxidation peak current of 4-AP. (c) The effect of pH on the reduction peak current of PR and 4-AP.

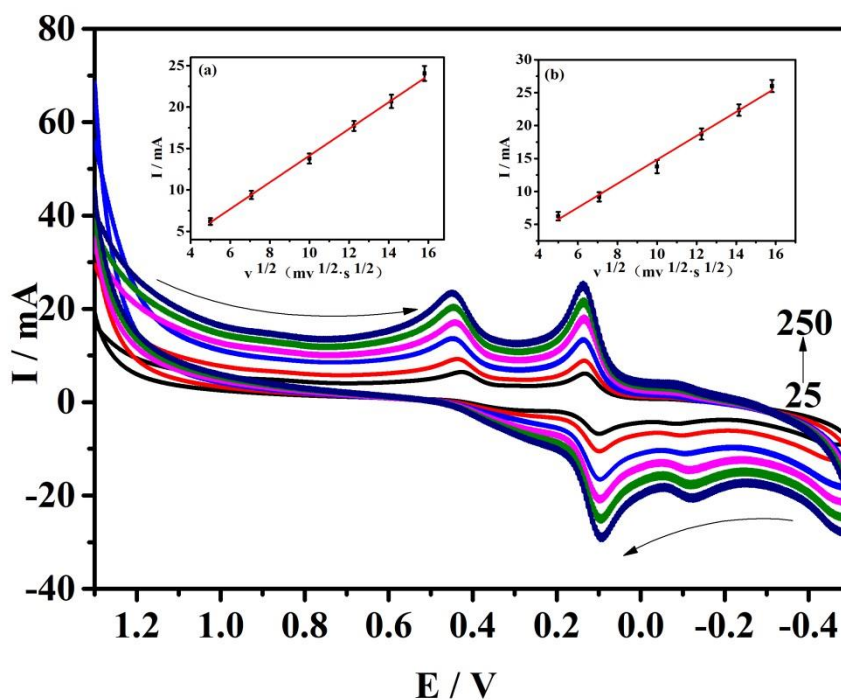


Figure S10. Cyclic voltammograms simultaneously measured at different scan rates. Test conditions: the voltage range from -0.5 to 1.3 V, pH of PBS buffer solution was 7, change the scan rate to test. (From inside to outside were 25, 50, 100, 150, 200, 250 $\text{mV}\cdot\text{s}^{-1}$); the inset (a) was the relationship between the oxidation peak current of PR and $v^{1/2}$, the inset (b) was the relationship between the oxidation peak current of 4-AP and $v^{1/2}$.

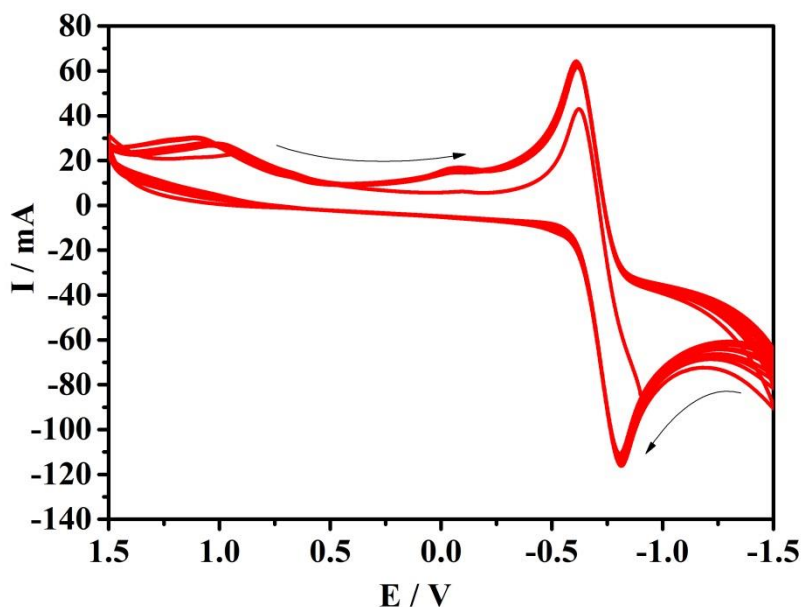


Figure S11. Cyclic voltammogram of modified electrode prepared by C1; C1 was dissolved in dimethyl sulfoxide (DMSO) and configured into $0.01 \text{ mol}\cdot\text{L}^{-1}$ solution. Test conditions: potential range from -1.5 to 1.5 V, scanning rate was $50 \text{ mV}\cdot\text{s}^{-1}$, number of scans was 20.

Table S1 Interference experiment of inorganic ions and organic compounds in paracetamol tablets on simultaneous determination of PR and 4-AP

Substance	Multiple (mass ratio)	Relative error
Sodium dodecyl sulfate	50	4.1 %
Starch	50	3.6 %
Na_2CO_3	100	4.6 %
CaCl_2	50	4.3 %
Dextrin	50	4.2 %

Table S2 The results of PR and 4-AP in paracetamol tablets

Sample s	Detected (μM)		RSD (%)	Added (μM)		Found (μM)		Recovery (%)	
	PR	4-AP		PR	4-AP	PR	4-AP	PR	4-AP
1	10.1	0		15.0	25.0	25.4	24.9	101.2	99.6
2	9.6	0		15.0	25.0	24.8	24.7	100.8	98.8
3	10.0	0	4.92	15.0	25.0	24.7	25.1	98.8	100.4
4	9.8	0		15.0	25.0	24.9	24.6	100.4	98.4
5	8.9	0		15.0	25.0	23.6	25.4	98.7	101.6

References

1. Y.R. Shi, and X.F. Ji, *Pharmaceut. Chem.*, 43 (2017) 180.
2. W.B. Zou, L.H. Yin, and S.H. Jin, *J. Pharmaceut. Biomed.*, 147 (2018) 81.
3. M. Shalini, J. Sirijagan, and G.K. Krishnapillai, *Talanta*, 179 (2018) 668.
4. H.J. Wang, S.Y. Zhang, S.F. Li, and J.Y. Qu, *Talanta*, 178 (2018) 188.
5. T. Nemeth, P. Jankovics, J. Nemeth-Palotas, and H. Koszegi-Szalai, *J. Pharmaceut. Biomed.*, 47 (2008) 746.
6. K. Asadpour-Zeynali, S. Maryam Sajjadi, and F. Taherzadeh, *Spectrochimica. Acta. A.*, 153 (2016) 674-680.
7. A. Merrikhi Khosroshahi, F. Aflaki, N Saemiyan, A. Abdollahpour, and R. Asgharian, *J. Pharm. Health. Sci.*, 4 (2016) 61.
8. L.A. Lammers, R. Achterbergh, M.C.M. Pistorius, J.A. Romijn, and R.A.A. Mathôt, *Ther. Drug. Monit.*, 39 (2017) 1.
9. A.R. Khaskheli, J. Fischer, J. Barek, V. Vyskocil, Sirajuddin, and M.I. Bhangar, *Electrochim. Acta*, 101 (2013) 238.
10. G. Burgot, F. Auffret, and J.L. Burgot, *Anal. Chim. Acta*, 343 (1997) 125.
11. Q. Chu, L. Jiang, X. Tian, and J. Ye, *Anal. Chim. Acta*, 606 (2008) 246.
12. A.B. Moreira, H.P.M. Oliveira, T.D.Z. Atvars, I.L.T. Dias, G.O. Neto, E.A.G. Zagatto, and L.T. Kubota, *Anal. Chim. Acta*, 539 (2005) 257.
13. F. Saadoune, S. Belouafa, M. Charrouf, A. Abourriche, A. Bennamara, and T. Ainane, *Am. Surgeon.*, 6 (2014) 191.
14. Sirajuddin, A.R. Khaskheli, A. Shah, M.I. Bhangar, A. Niaz, and S. Mahesar, *Spectrochim. Acta. A.*, 68 (2007) 747.
15. S. Biswas, D. Chakraborty, R. Das, R. Bandyopadhyay, and P. Pramanik, *Anal. Chim. Acta*, 82 (2015) 98.
16. J.D.R.M. Neto, W.D.R. Santos, P.R. Lima, S.M.C.N. Tanaka, A.A. Tanaka, and L.T. Kubota, *Sensor. Actuat. B-Chem.*, 152 (2011) 220.
17. P. Rattanarat, A. Suea-Ngam, N. Ruecha, W. Siangproh, C.S. Henry, M. Srisa-Art, and O. Chailapakul, *Anal. Chim. Acta*, 925 (2016) 51.
18. F.Y. Kong, S.X. Gu, J.Y. Wang, H.L. Fang, and W. Wang, *Sensor. Actuat. B-Chem.*, 213 (2015) 397.
19. P. K. Kalambate, B.J. Sanghavi, S.P. Karna, and A.K. Srivastava, *Sensor. Actuat. B-Chem.*, 213 (2015) 285.
20. H. Wang, Z. Liu, Q.Q. Liang, G.C. Han, P. Guo, X.Q. Lao, S.F. Zhang, Z.C. Chen, and R.S. Zeng, *Int. J. Electrochem. Sci.*, 13 (2018) 10454.
21. H. Filik, S. Aydar, and A.A. Avan, *Anal. Lett.*, 48 (2015) 2581.
22. H.S. Yin, K. Shang, X.M. Meng, and S.Y. Ai, *Microchim. Acta*, 175 (2011) 39.
23. H.S. Yin, X.M. Meng, Z.N. Xu, L.J. Chen, and S.Y. Ai, *Anal. Methods-UK*, 4 (2012) 1445.
24. L.Y. Shiroma, M. Santhiago, A.L. Gobbi, and L.T. Kubota, *Anal. Chim. Acta*, 725 (2012) 44.
25. T. Thomas, R.J. Mascarenhas, F. Cotta, K.S. Guha, B.E.K. Swamy, P. Martis, and Z. Mekhalif, *Colloid. Surface. B.*, 101 (2013) 91.
26. P. Guo, Z. Liu, Y.J. Guo, J.H. Xia, H.H. Wei, and F.S. Tang, *China Food Additives*, 12 (2015) 140.
27. J. Shi, M.X. Xu, Q.H. Tang, K. Zhao, A.P. Deng, and J.G. Li, *Spectrochimica. Acta. A.*, 191 (2018) 1.
28. C. Shiju, D. Arish, N. Bhuvanesh, and S. Kumaresan, *Spectrochimica. Acta. A.*, 145 (2015) 213.
29. J. Yu, X.B. Jia, and W.S. Zhao, *Chemical Research*, 27 (2016) 779.
30. K. Divya, G.M. Pinto, and A.F. Pinto, *J. Int. Pharm. Res.*, 9 (2017) 27.
31. A.M. Abu-Dief, and I.M.A. Mohamed, *Beni-Suef University Journal of Basic and Applied Sciences*, 4 (2015) 119.
32. U. Divya, Vibha, S. Sarbjit, and K. Manpreet, *Current. Bioactive. Compounds*, 11 (2015) 215.

33. K.T. Tadele, *J. Pharm. Med. Res.*, 1 (2017) 73.
34. L.T. Wang, Y. Zhang, Y.L. Du, D.B. Lu, Y.Z. Zhang, and C.M. Wang, *J. Solid. State. Electrochem.*, 16 (2012) 1323.
35. F. Yuan, H.M. Zhao, M. Liu, and X. Quan, *Biosens. Bioelectron.*, 68 (2015) 7.
36. S. Mehretie, S. Admassie, T. Hunde, M. Tessema, and T. Solomon, *Talanta*, 85 (2011) 1376.
37. K. Bharathi, S.P. Kumar, P.S. Prasad, and V. Narayanan, *Mater Today*, 5 (2018) 8961.
38. M. Köse, G. Ceyhan, M. Tümer, I. Demirtas, I. Gönül, and V. McKee, *Spectrochimica. Acta. A.*, 137 (2015) 477.
39. S.P. Kumar, R. Suresh, K. Giribabu, R. Manigandan, S. Munusamy, S. Muthamizh, and V. Narayanan, *Spectrochimica. Acta. A.*, 139 (2015) 431.
40. M. Ni, J.X. Li, Y.C. Fan, H.C. Wei, and X.Q. Zhang, *Chemical Reagents*, 38 (2016) 1051.
41. P. Gull, B.A. Babgi, and A.A. Hashmi, *Microb. Pathogenesis*, 110 (2017) 444.
42. X.K. Shi, S.S. Mao, K.S. Shen, H.L. Wu, and X. Tang, *J. Coord. Chem.*, 70 (2017) 2015.
43. S. Ramezani, M. Pordel, and A. Davoodnia, *Inorg. Chim. Acta*, 484 (2019) 450.
44. W.H. Mahmoud, R.G. Deghadi, and G.G. Mohamed, *Res. Chem. Intermed.*, 42 (2016) 7869.
45. B. Bouzerafa, D. Aggoun, Y. Ouenoughi, A. Ourari, R. Ruiz-Rosas, E. Morallon, M.S. Mubarak, *J. Mol. Struct.*, 1142 (2017) 48.
46. N.A. Karim, and S.K. Kamarudin, *J. Electroanal. Chem.*, 803 (2017) 19.
47. S.P. Kumara, K. Giribabu, R. Manigandan, S. Munusamy, S. Muthamizh, A. Padmanaban, T. Dhanasekaran, R. Suresh, and V. Narayanan, *Electrochim. Acta*, 194 (2016) 116.
48. E. Laviron, *J. Electroanal. Chem.*, 52 (1974) 355-393.
49. H.Y. Zhai, Z.X. Liang, Z.G. Chen, H.H. Wang, Z.P. Liu, Z.H. Su, and Q. Zhou, *Electrochim. Acta*, 171 (2015) 105.
50. W.C. Zhu, H. Huang, X.C. Gao, and H.Y. Ma, *Mat. Sci. Eng. C.*, 45 (2014) 21.
51. M. Zidan, R.M. Zawawi, M. Erhayem, and A. Salhin, *Int. J. Electrochem. Sci.*, 9 (2014) 7605.
52. Z. Guo, D.D. Li, X.K. Luo, Y.H. Li, Q.N. Zhao, M.M. Li, Y.T. Zhao, T.S. Sun, and C. Ma, *J. Colloid. Interface. Sci.*, 490 (2017) 11.
53. S. Sharma, S.K. Khanna, J. Singh, and S. P. Satsangee, *Oriental. J. Chem.*, 31 (2017) 201.

© 2019 The Authors. Published by ESG (www.electrochemsci.org). This article is an open access article distributed under the terms and conditions of the Creative Commons Attribution license (<http://creativecommons.org/licenses/by/4.0/>).